frontiers in Energy Research

BRIEF RESEARCH REPORT
published: 14 April 2021
doi: 10.3389/fenrg.2021.658270

Charge Carrier Dynamics in Sn-Doped Two-Dimensional Lead Halide Perovskites Studied by Terahertz Spectroscopy

Zhengyuan Qin[1], Chunfeng Zhang[1], Lan Chen[1], Xiaoyong Wang[1] and Min Xiao[1,2]*

[1] National Laboratory of Solid State Microstructures, School of Physics, and Collaborative Innovation Center for Advanced Microstructures, Nanjing University, Nanjing, China, [2] Department of Physics, University of Arkansas, Fayetteville, AR, United States

Sn doping is established as an effective approach to promote the light emission properties in in two-dimensional lead-halide perovskites. However, the effect on the charge carrier dynamics is largely unexplored. In this work, we conduct terahertz spectroscopy to study the effects of Sn doping on the charge dynamics in the two-dimensional perovskites $PEA_2Sn_xPb_{1-x}I_4$ (PEA = phenethylammonium) with different doping levels. The spectral dispersion analysis suggests that the early-stage dynamics with lifetime of $\sim$ 2 ps is contributed by both the transport of hot charge carriers and the polarizability of hot excitons. The long-lived component of first-order charge carrier recombination is dramatically improved when Sn doping increases, which is ascribed to the equilibrium between charge carriers and excitons with smaller bind energies in the higher-level Sn-doped samples. The finding in this work suggests Sn doping is an effective approach to optimize the charge carrier transport in 2D perovskite for potential optoelectronic applications.

Keywords: 2D perovskites, Sn doping, charge carriers, self-trapped excitons, THz spectroscopy

OPEN ACCESS

Edited by:
Letian Dou,
Purdue University, United States

Reviewed by:
Yongping Fu,
Columbia University, United States
Mengxia Liu,
University of Cambridge, United Kingdom

****Correspondence:***
Chunfeng Zhang
cfzhang@nju.edu.cn

Specialty section:
This article was submitted to Solar Energy, a section of the journal Frontiers in Energy Research

Received: *25 January 2021*
Accepted: *19 March 2021*
Published: *14 April 2021*

Citation:
Qin Z, Zhang C, Chen L, Wang X and Xiao M (2021) Charge Carrier Dynamics in Sn-Doped Two-Dimensional Lead Halide Perovskites Studied by Terahertz Spectroscopy. Front. Energy Res. 9:658270. doi: 10.3389/fenrg.2021.658270

INTRODUCTION

Two-dimensional (2D) lead-halide perovskites have become increasingly prevalent in the past few years due to its high performance in optoelectronics devices with increased stability in ambient condition (Ishihara et al., 1990; Smith et al., 2014; Wang et al., 2016; Yuan et al., 2016; Grancini and Nazeeruddin, 2019; Ke et al., 2019; Blancon et al., 2020). In comparison with the 3D counterparts, light emission efficiency is markedly enhanced because the electron-hole pairs are strongly bounded benefiting from the strong quantum size confinement. The merit suggests the 2D perovskites are particularly suitable for application of light-emitting diodes (LEDs). In 2D perovskites, a broadband emission with large stokes shift is also observed, which is proposed for the potential applications of white light display and lightening (Dohner et al., 2014a,b; Smith et al., 2017; Smith and Karunadasa, 2018; Li C. et al., 2020). In addition to efficient light emission, the transport of charge carriers is also pivotal for the performance of an optoelectronic device which, however, is limited in 2D perovskites.

Element doping is a common strategy to detune the electronic and optical properties for modern semiconductor-based optoelectronic technology (Norris et al., 2008; Schubert, 2015). For

perovskite semiconductors, the bandgaps in the visible range can be controlled by halide element engineering (Noh et al., 2013; Protesescu et al., 2015). Sn doping at the site of lead, originally proposed to reduce the heavy metal of lead, has been established as an efficient approach to extend the absorption coverage to the long wavelength range, which is particularly important for tandem solar cells (Hao et al., 2014; Lin et al., 2019; Klug et al., 2020). In 2D perovskites, the broadband emission is generally weak at room temperature, which is dramatically promoted by Sn doping (Yu et al., 2019; Zhang et al., 2019). The broadband emission has been assigned to the extrinsic self-trapped excitons (STE) due to efficient electron-phonon coupling and low-dimensionality structure (Hu et al., 2016; Li S. et al., 2019; Li T. et al., 2019; Wang et al., 2019; Li J. et al., 2020). Nevertheless, it remains poorly explored how these Sn doping affect the transport of charge carriers in the 2D perovskites.

In this work, we study the dynamics of charge carriers in two-dimensional perovskites $PEA_2Sn_xPb_{1-x}I_4$ (PEA = phenethyl ammonium) with different level of Sn doping (<10%) using optical-pump-Terahertz-probe (OPTP) spectroscopy. The recombination dynamics exhibit three exponential decay components with characterized lifetimes of ∼ 2 ps, 30–50 ps, and ∼ 1 ns, respectively. The lifetimes of short-lived (∼ 2 ps) and long-lived (∼ 1 ns) components are independent of pump fluence, while the second recombination process (30 ∼ 50 ps) is related to the bimolecular recombination. The proportion of long-lived component (∼ 1 ns) is dramatically improved with increasing the level of Sn doping, which can be understood as the equilibrium between the charge carriers and bounded electron-hole pairs with reduced binding energy in the samples with higher level Sn doping. Such a scenario has been confirmed by temperature-dependent measurements. The spectral dispersion of short-lived component shows significant disparity from that of free charge response, which is argued to be contributed by both of the transport of hot charge carriers and polarizability of hot excitons. The charge carrier dynamics uncovered in the Sn-doped 2D perovskites implies a critical role of ultrafast hole trapping process for the STE. The finding in this work suggests Sn doping is an effective approach to optimize the charge carrier transport in 2D perovskite for potential optoelectronic applications.

RESULTS AND DISCUSSION

We study the dynamics of charge carriers in thin film samples of 2D perovskite $PEA_2Sn_xPb_{1-x}I_4$ with five different doping levels (x = 0%, 0.1%, 1%, 5%, 10%). The samples are prepared using literature procedure as described in the section of "Methods." To minimize the degradation due to the oxidation of Sn^{2+}, sample preparation has been carried out in a glove box filled with argon atmosphere. The samples were prepared on the z-cut quartz substrates and then mounted onto the cold finger of an optical cryostat where the vacuum is established for optical measurements.

We monitor the dynamics of photo-induced charge carriers using OPTP spectroscopy as shown in **Figure 1A**. The probe beam of THz radiation is generated from a ZnTe nonlinear crystal with ultrashort pulse based on the optical rectification effect. The second-harmonic generation of the fundamental beam at 400 nm is employed as the pump beam to excite the samples. The dynamics of charge carriers is manifested as photo-induced THz transmission changes ($-\Delta E/E$) of the samples. The experimental data of THz response can be calculated with the photoconductivity ($\Delta\sigma$) in the frequency range 0.3–1.5 THz. Moreover, the decay dynamics of charge carriers can be captured by measuring the THz response as a function of the time delay between the optical pump and THz probe pulses.

For free charge carriers, the value of $-\Delta E/E$ is proportional to the photoconductivity ($\Delta\sigma$), which is linearly dependent on the product of the density (N) and mobility (μ) of photogenerated carriers (Ulbricht et al., 2011). The spectral response of free charge carriers can be described using the celebrated Drude-Smith model. Resonance features with Lorentz spectral profiles may also be recorded if the frequencies of phonon resonances are in the probe spectral range (Wang et al., 2006; V Laarhoven et al., 2008; Cinquanta et al., 2019; Kumar et al., 2020). In addition, the polarizability of photo-excited bounded electron-hole pairs (i.e., excitons) may cause the THz response with a phase shift of the $\Delta E(t)$ waveform (Kumar et al., 2020). The THz responses of free charge carriers and exciton can be distinguished by their different waveforms.

Figure 1B shows a typical trace of THz transmission change ($-\Delta E/E$) measured in a sample of 2D perovskite with 1% Sn doping. Phenomenologically, the decay trace can be reproduced by a function with three exponential components, i.e., $f(t) = A_1e^{t/\tau_1} + A_2e^{t/\tau_2} + A_3e^{t/\tau_1}$. The lifetime parameters of the three components are $\tau_1 \sim 2$ ps, $\tau_2 \sim 40$ ps, and $\tau_3 \sim 1$ ns, respectively. The values of τ_1 and τ_3 are nearly independent of the pump fluence while the value of τ_2 is sensitive to the pump fluence (**Supplementary Figure 2** and **Supplementary Table 1**). The results suggest that bimolecular recombination is involved in the charge carrier dynamics on the timescale of tens of picoseconds (Thouin et al., 2018). To gain more insights about the components characterized with lifetime parameters of τ_1 and τ_3, we compare the waveforms of THz responses recorded at the time delays of 0 and 500 ps and analyze the spectral dispersion of the optical conductivity (**Figures 1C–E**), respectively. For the slow component, the THz response can be well-reproduced by the Drude-Smith model (**Figure 1E**), indicating the dominant contribution from the free charge carriers. The lifetime of ∼ 1 ns is a first-order recombination process with lifetime limited by the defect trapping process (Wehrenfennig et al., 2014). The THz response at the early stage is more complicated. The peak of THz waveform change is close to that of incident THz pulse, which is consistent with the contribution from charge carriers. Nevertheless, the spectral dispersion shows a significant disparity from the Drude-Smith model. The imaginary part of photoconductivity ($\Delta\sigma_2$) exhibits a marked divergence from the curve simulated using the best fitting parameters for the real part ($\Delta\sigma_1$) (**Figure 1D**). Such a deviation can be explained as contributions from both the charge carrier transport and exciton polarizability. Upon optical pump at 400 nm, both excitons and charge carriers are excitable in the 2D perovskites. The real part of photo-induced THz conductivity

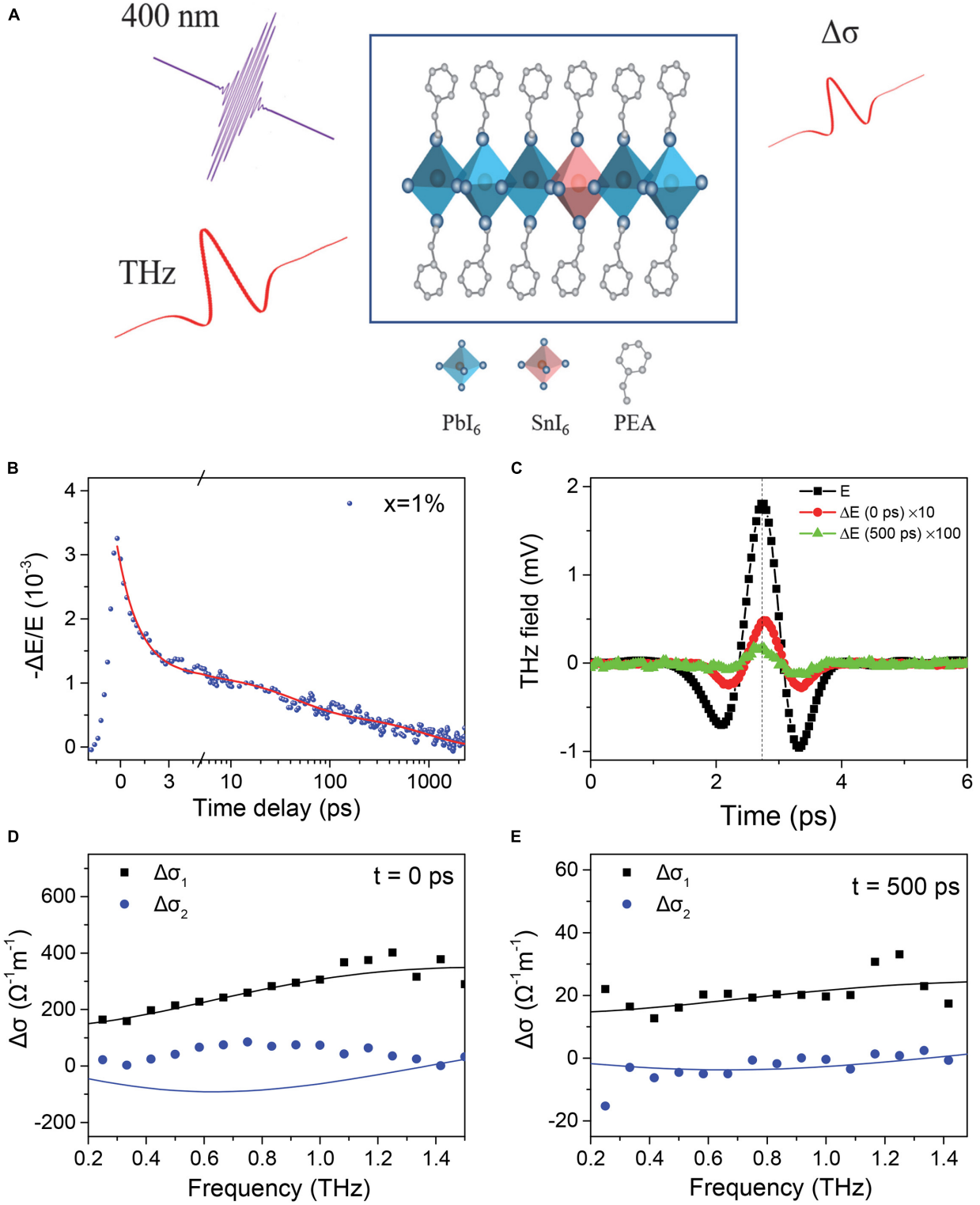

FIGURE 1 | (A) Schematic of OPTP measurements in Sn-doped 2D perovskites. The dynamics of charge carriers is probed by measuring photo-induced photoconductivity change ($\Delta\sigma$) in the THz spectral domain. **(B)** The time-dependent trace of THz transmission change ($-\Delta E/E$) recorded from a 2D perovskite sample of $PEA_2Sn_xPb_{1-x}I_4$ (x = 1%) with pump at 400 nm of 10 $\mu J/cm^2$ (excitation density of $\sim 8 \times 10^{17}$ cm^{-3}) The decay trace can be reproduced by a function with three exponentially decay components. **(C)** The photo-excited change of THz waveform at the time delays of 0 and 500 ps is compared with the probe THz spectrum, respectively. The calculated spectra of complex $\Delta\sigma$ at the delays of 0 **(D)** and 500 ps **(E)** are compared with the fitting curves through the Drude-Smith model.

($\Delta\sigma_1$) is primarily contributed by the charge carriers while the imaginary part ($\Delta\sigma_2$) is induced by the exciton polarizability. The "hot" charge carriers and excitons undergo a cooling process with excess energy loss through carrier-phonon inelastic scattering, resulting in a decrease in photoconductivity and a change in exciton polarizability, which is primarily responsible for the fast decay component. Such an assignment is consistent with the dependence of charge carrier dynamics on the pump fluence. The decay lifetime of the early stage seems not to be sensitive to pump fluence, which is likely caused by the fact that the hot excitons make the major contribution of THz conductivity. The lifetime of the fast component is primarily determined by the process of exciton-phonon scattering, i.e., the cooling process (Burgos-Caminal et al., 2020). The Auger recombination due to exciton-exciton scattering is much slower with insignificant impact on the early-stage dynamics. Other than that, the decay lifetime of the slow component becomes faster with increasing pump fluence, which is an evidence of carrier-carrier scattering. In addition, the amplitude ratio of the faster component increases with increasing pump fluence as summarized in **Supplementary Table 1**.

Dynamic behaviors with three exponential decay components are also observed in the samples with different Sn doping levels (**Figure 2A**), suggesting a similar mechanism underlying the charge carrier dynamics in these samples. Nonetheless, the amplitudes and the lifetimes of these components show notable Sn-doping dependences (**Figures 2B,C**). With increasing Sn doping level, the initial photoconductivity of 2D perovskites decreases but the amplitude of the slow component increases. As the absorption coefficients of the samples are similar at the pump wavelength of 400 nm, the variation of the initial is possibly caused by the different mobilities (μ) of the hot carriers in these samples. Normally, introducing defects will increase the probability of scattering and reduce the mobility of charge carriers, which may explain the decrease of the initial signal amplitude with increasing Sn doping level (Parkinson et al., 2007; Richter and Schmuttenmaer, 2010). The amplitude changes of the long-lived components are possibly related to the equilibrium shift between the excitons and free charge carriers. Thermodynamically, the equilibrium is established after several ps. The proportion of free charges (η) can be estimated by the Saha equation as (Gélvez-Rueda et al., 2017; Burgos-Caminal et al., 2020)

$$\frac{\eta^2}{1-\eta} = \frac{2\pi\mu k_B T}{nh^2} e^{E_b/k_B T} \quad (1)$$

where E_b is the exciton binding energy, k_B is the Boltzmann constant, T is the temperature, h is the Planck constant, and n is the excitation density (Gélvez-Rueda et al., 2017). With Sn doping increasing, bounded excitation complex related to the structure imperfections may be formed with binding energies smaller than that of the intrinsic excitons. The increased long-term photoconductivity is owing to the small detrapping barriers of the trapped excitons related to the Sn doping. Within the scenario, the proportion of free charges increases with increasing Sn doping in the 2D perovskites, which explains the dependence of Sn doping on the charge carrier dynamics.

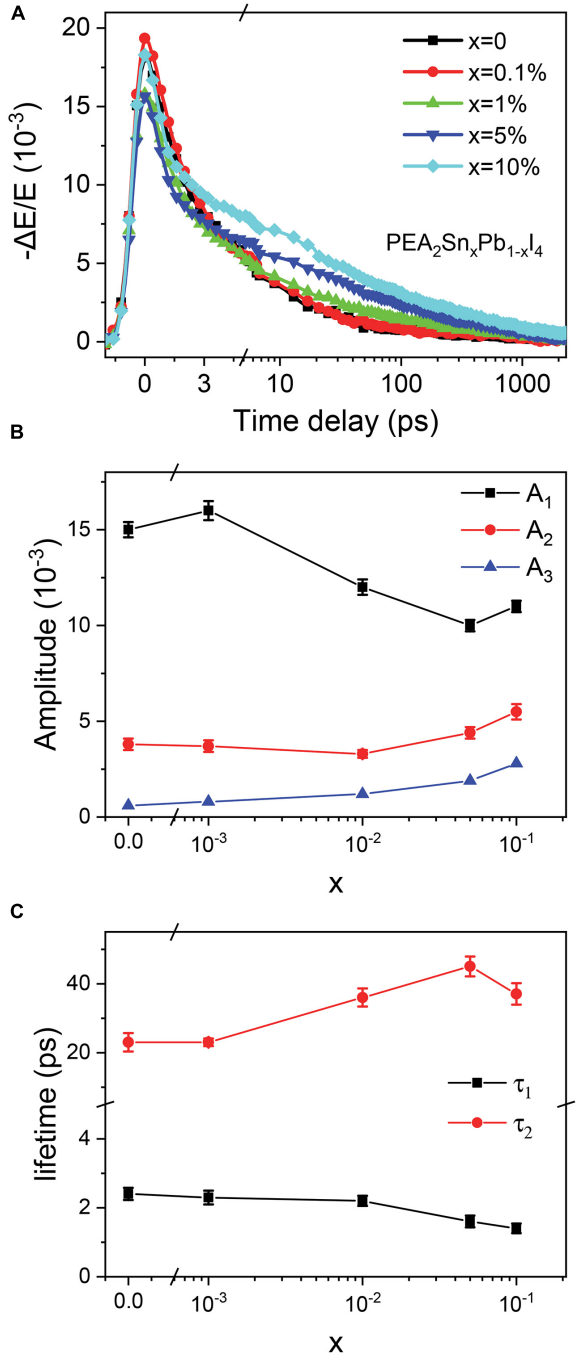

FIGURE 2 | Doping-level-dependent charge carrier dynamics in Sn-doped PEA_2PbI_4 perovskite samples. **(A)** The traces of OPTP decay dynamics recorded from the samples with different doping levels at room temperature with pump of 50 $\mu J/cm^2$. The fitting parameters of amplitudes **(B)** and lifetimes **(C)** derived from the tri-exponential decay function are plotted vs. the doping levels.

To confirm the above explanation, we study the temperature dependence of the charge carriers in these samples from 80 to 300 K. **Figures 3A–C** and **Supplementary Figure 3** show the THz

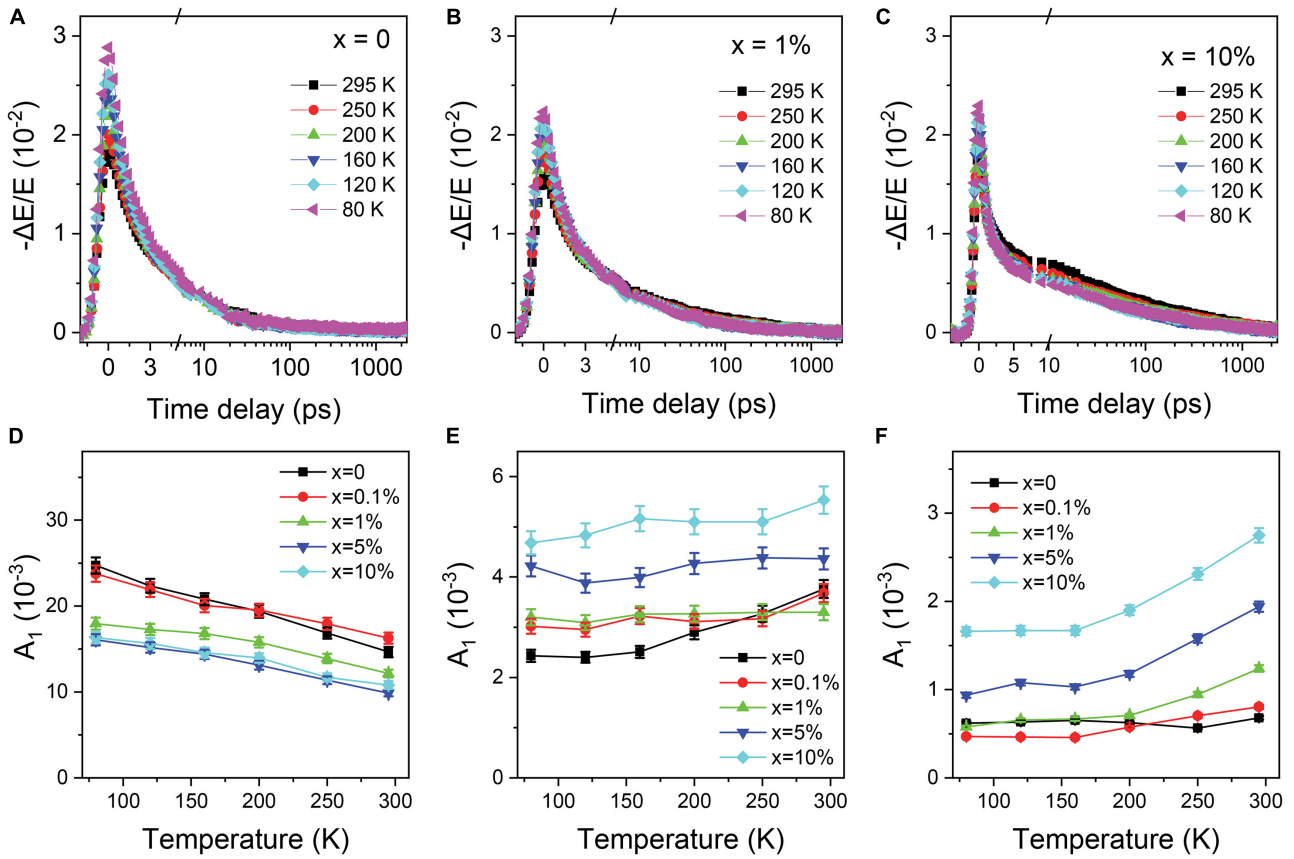

FIGURE 3 | Temperature-dependent charge carrier dynamics in the samples with different doping levels. The decay dynamics of the samples with Sn-doping level of $x = 0$ **(A)**, $x = 1\%$ **(B)**, and $x = 10\%$ **(C)** at different temperatures. Temperature-dependent fitting amplitudes of the three components of **(D)** A_1, **(E)** A_2, and **(F)** A_3, respectively.

traces illustrating the decay dynamics of $PEA_2Sn_xPb_{1-x}I_4$ samples with different doping levels. With increasing temperature, the amplitude of initial photoconductivity drops due to increased momentum scattering of the charge (**Figure 3D**; Karakus et al., 2015; Milot et al., 2015). In the samples with higher level doping of Sn, the long-lived components increase with increasing temperature, implying more charge carriers are activated thermally (**Figures 3E,F**). Such temperature-dependent behaviors are consistent with smaller binding energies in higher level Sn-doped perovskite samples according to Saha equation. These data show that the charge carrier dynamics is tightly associated to the Sn doping which is valuable for optimizing the charge transport for optoelectronic applications. Hole doping induced by tin vacancies may significantly reduce the carrier lifetime, which is probably caused by the oxidation of Sn^{2+} (Lin et al., 2019). To minimize such an effect, the sample preparations and optical measurements have been carried out in the nitrogen atmosphere or vacuum. The effect of hole doping induced by tin vacancies has been insignificant which is confirmed by the charge dynamics in the film of pure PEA_2SnI_4 (**Supplementary Figure 4**).

The Sn-doping-dependent dynamics of charge carriers may shine some light into the mechanism underlying the light emission in these samples. **Figure 4A** show time-integrated PL spectra of $PEA_2Sn_xPb_{1-x}I_4$ with different doping levels recorded at room temperature. Without Sn doping, PL from the pure PEA_2PbI_4 sample shows a narrowband near-band-edge emission around 525 nm. With increasing the doping level to 1%, the band-edge emission decreases while a broadband emission emerges. Such a broadband emission in 2D perovskites has been explained as the defect emission and/or the extrinsic STE. With further increasing doping of Sn, the intensity of broadband emission decreases with slight blue shift of emission peak (**Figure 4B**). These results are consistent with the results reported previously (Yu et al., 2019). Time-resolved PL (TRPL) spectra show that the broadband emission is related to the quenching of band-edge emission (**Figures 4C,D**). When Sn doping is introduced, the lifetime of band-edge emission is dramatically shortened due to the fast-trapping process. Interestingly, the band-edge emission shows a slow rise with time scale of hundreds of ps in the low doping range (<1%), which possibly represents the formation dynamics of extrinsic STE, which is consistent with the PL excitation spectrum (**Supplementary Figure 5**). Self-trapping process causes transient lattice distortions after photoexcitation. The charge carrier dynamics uncovered by the OPTP measurements suggest the long-lived component of

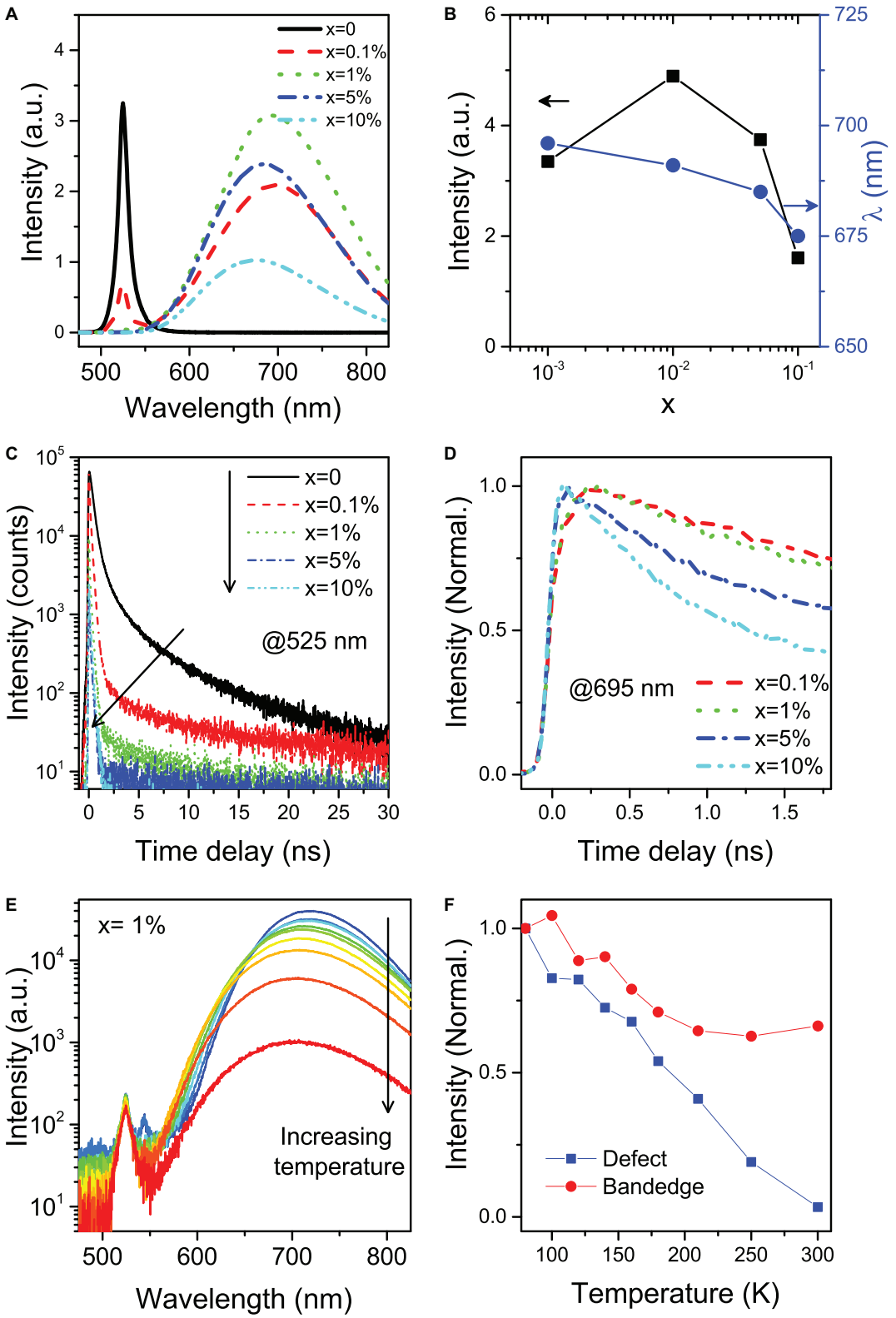

FIGURE 4 | PL emission from Sn-doped PEA_2PbI_4 perovskites. **(A)** PL spectra from the samples with different doping levels at room temperature. **(B)** The emission intensities and peak wavelengths of the broadband emissions recorded from the samples with different doping levels. PL decay curves of the samples probed at 525 nm **(C)** and 695 nm **(D)**, respectively. **(E)** PL spectra recorded from an 1% Sn-doped sample. **(F)** Temperature-dependent intensities of emission at 525 and 695 nm plotted normalized to the values at 80 K.

free charges is tiny in the samples with 1% Sn doping or less. Nonetheless, doping-related broadband emission shows a remarkable high quantum efficiency in the Sn-doped perovskite samples. This result suggests that self-trapping of free charges on the time scale of hundreds of ps should not be the major formation channel of the STEs. Alternatively, as suggested in a previous report (Li T. et al., 2019), the formation of STE is likely induced by the formation of self-trapped holes causing transient lattice distortions and the trapping process of electrons via Coulomb interaction at the time scale of hundreds of ps. With introduction of Sn, the photogenerated holes are possibly localized at the Sn site on the picosecond timescale, resulting in the decrease of initial photoconductivity. The electrons are trapped to the Sn site slowly instead of relaxation through free-exciton recombination, leading to the increasing proportion of charge-trapping process. In addition to the STE, more defect-liked excitations are also possibly formed especially in the samples with higher level Sn doping. In the doping range, the mixed Sn-Pb phase is possibly formed resulting in high density of defect states. The reversal process of self-trapping or defect trapping contributes to the THz conductivity of the measured samples. This is consistent with the temperature-dependent PL emission in Sn-doped 2D perovskites (**Figures 4E,F**). With increasing temperature, the proportion of free charges is thermally activated from the trapped states, leading to the reduced broadband emission.

CONCLUSION

In summary, the effects of Sn doping on the charge carrier dynamics in two-dimensional lead halide perovskites have been studied using OPTP measurements. The decay dynamics is featured with a fast component of hot carrier response ($\sim$ 2 ps) and a long-lived component of first-order recombination ($\sim$ 1 ns). The early-stage dynamics is contributed by the hot free charges and exciton polarizability, which is insensitive to the Sn doping level. The long-lived component is markedly increased when the Sn-doping level increases, which is ascribed to the decreased binding energy of exciton complex in the high-level doped samples as supported by the temperature-dependent measurements. The equilibrium between the bounded excitation complex and free charges are responsible for the light emission and charge carrier dynamics. The finding in this working suggests Sn-doping is a promising strategy to optimize the charge carrier transport for 2D perovskite devices.

METHODS

Materials

N, N-dimethylformamide (DMF, anhydrous, purity ∼99.8%), Lead iodide (PbI_2, purity ∼99.99%) and Tin(II) iodide (SnI_2, purity ∼99.99%) were purchased from Sigma-Aldrich. 2-phenylethanamine iodide (PEAI) was purchased from Xi'an Polymer Light Technology Corp (Xi'an, China). All the chemicals were used without further purification.

Preparation of 2D Perovskite Film

Perovskite films were spin-coated in a glove box. Quartz substrates were thoroughly cleaned by sequential ultrasonic treatment in detergent, acetone, deionized water and acetone. Organic residue was further removed by treating with UV-ozone for 30 min. Stoichiometric amounts of PbI_2 and PEAI were dissolved in anhydrous DMF to form PEA_2PbI_4 precursor solution (1M). For PEA_2SnI_4 precursor solution, PbI_2 was replaced by SnI_2. The precursor solutions were stirred for 2 h and filtered through a syringe filter (0.45 μm). Afterward, preheated solutions (70°C) were spin coated on preheated substrates (100°C) at a speed of 3,000 rpm for 40 s. The resultant films were further heated at 100°C for 10 min. Sn-doped films were obtained by mixing two solution precursors according to the contents.

Optical-Pump Terahertz-Probe Spectroscopy (OPTPS)

A commercial Ti:Sapphire regenerative amplifier (Libra, Coherent) at 800 nm with a pulse duration of 90 fs, and repetition rate of 1 kHz was used to generate THz radiation via optical rectification in a 1 mm thick ZnTe(110) nonlinear crystal and detect it using free space electro-optic sampling in a 1 mm thick ZnTe(110) nonlinear crystal. The second harmonic generation (SHG) at 400 nm was generated to excite the perovskite thin films deposited on z-cut quartz substrates. The time delay between the 400-nm optical pump pulse and THz probe pulse was enabled by a translation stage. The samples were mounted in the cryostat (MicrostatHe, Oxford) for temperature-dependent experiments. All the measurements were conducted in a nitrogen-purged environment to avoid the effects of water vapor absorptions in the ambient air.

PL Spectroscopy

The PL spectra were recorded by a liquid nitrogen cooled charge-coupled device (PyLoN:400B, Princeton Instruments) mounted on a monochromator (Acton SP2500, Princeton Instruments). PL decay dynamics were measured by time-correlated single-photon counting (PicoHarp 300, Picoquant) under the 405 nm pulsed excitation (LDH-D-C-405M, Picoquant) with a repetition rate of 2.5 MHz.

DATA AVAILABILITY STATEMENT

All datasets generated for this study are included in the article/**Supplementary Material**, further inquiries can be directed to the corresponding author/s.

AUTHOR CONTRIBUTIONS

CZ, XW, and MX designed the projects. ZQ and LC prepared the samples and performed the optical measurements. ZQ and CZ analyzed the data. ZQ and CZ wrote the manuscript with the help

from all other authors. All authors contributed to the article and approved the submitted version.

FUNDING

This work was supported by the National Key R&D Program of China (Grant Nos. 2017YFA0303700 and 2018YFA0209101), the National Science Foundation of China (Grant Nos. 21922302, 21873047, 11904168, 91833305, 91850105), the Priority Academic Program Development of Jiangsu Higher Education Institutions (PAPD), and the Fundamental Research Funds for the Central University. CZ acknowledges financial support from Tang Foundation.

SUPPLEMENTARY MATERIAL

The Supplementary Material for this article can be found online at: https://www.frontiersin.org/articles/10.3389/fenrg.2021.658270/full#supplementary-material

REFERENCES

Blancon, J.-C., Even, J., Stoumpos, C. C., Kanatzidis, M. G., and Mohite, A. D. (2020). Semiconductor physics of organic–inorganic 2D halide perovskites. *Nat. Nanotechnol.* 15, 969–985. doi: 10.1038/s41565-020-00811-1

Burgos-Caminal, A., Socie, E., Bouduban, M. E., and Moser, J.-E. (2020). Exciton and carrier dynamics in two-dimensional perovskites. *J. Phys. Chem. Lett.* 11, 7692–7701. doi: 10.1021/acs.jpclett.0c02425

Cinquanta, E., Meggiolaro, D., Motti, S. G., Gandini, M., Alcocer, M. J., Akkerman, Q. A., et al. (2019). Ultrafast THz probe of photoinduced polarons in lead-halide perovskites. *Phys. Rev. Let.* 122:166601.

Dohner, E. R., Hoke, E. T., and Karunadasa, H. I. (2014a). Self-assembly of broadband white-light emitters. *J. Am. Chem. Soc.* 136, 1718–1721. doi: 10.1021/ja411045r

Dohner, E. R., Jaffe, A., Bradshaw, L. R., and Karunadasa, H. I. (2014b). Intrinsic white-light emission from layered hybrid perovskites. *J. Am. Chem. Soc.* 136, 13154–13157. doi: 10.1021/ja507086b

Gélvez-Rueda, M. C., Hutter, E. M., Cao, D. H., Renaud, N., Stoumpos, C. C., Hupp, J. T., et al. (2017). Interconversion between free charges and bound excitons in 2D hybrid lead halide perovskites. *J. Phys. Chem. C* 121, 26566–26574. doi: 10.1021/acs.jpcc.7b10705

Grancini, G., and Nazeeruddin, M. K. (2019). Dimensional tailoring of hybrid perovskites for photovoltaics. *Nat. Rev. Mater.* 4, 4–22. doi: 10.1038/s41578-018-0065-0

Hao, F., Stoumpos, C. C., Chang, R. P., and Kanatzidis, M. G. (2014). Anomalous band gap behavior in mixed Sn and Pb perovskites enables broadening of absorption spectrum in solar cells. *J. Am. Chem. Soc.* 136, 8094–8099. doi: 10.1021/ja5033259

Hu, T., Smith, M. D., Dohner, E. R., Sher, M.-J., Wu, X., Trinh, M. T., et al. (2016). Mechanism for broadband white-light emission from two-dimensional (110) hybrid perovskites. *J. Phys. Chem. Lett.* 7, 2258–2263. doi: 10.1021/acs.jpclett.6b00793

Ishihara, T., Takahashi, J., and Goto, T. (1990). Optical properties due to electronic transitions in two-dimensional semiconductors $(C_nH_{2n+1}NH_3)_2PbI_4$. *Phys. Rev. B* 42:11099. doi: 10.1103/physrevb.42.11099

Karakus, M., Jensen, S. A., D'angelo, F., Turchinovich, D., Bonn, M., and Canovas, E. (2015). Phonon–electron scattering limits free charge mobility in methylammonium lead iodide perovskites. *J. Phys. Chem. Lett.* 6, 4991–4996. doi: 10.1021/acs.jpclett.5b02485

Ke, W., Mao, L., Stoumpos, C. C., Hoffman, J., Spanopoulos, I., Mohite, A. D., et al. (2019). Compositional and solvent engineering in Dion–Jacobson 2D perovskites boosts solar cell efficiency and stability. *Adv. Energy Mater.* 9:1803384. doi: 10.1002/aenm.201803384

Klug, M. T., Milot, R. L., Patel, J. B., Green, T., Sansom, H. C., Farrar, M. D., et al. (2020). Metal composition influences optoelectronic quality in mixed-metal lead–tin triiodide perovskite solar absorbers. *Energy Environ. Sci.* 13, 1776–1787. doi: 10.1039/d0ee00132e

Kumar, A., Solanki, A., Manjappa, M., Ramesh, S., Srivastava, Y. K., Agarwal, P., et al. (2020). Excitons in 2D perovskites for ultrafast terahertz photonic devices. *Science Advances* 6:eaax8821. doi: 10.1126/sciadv.aax8821

Li, C., Yang, J., Su, F., Tan, J., Luo, Y., and Ye, S. (2020). Conformational disorder of organic cations tunes the charge carrier mobility in two-dimensional organic-inorganic perovskites. *Nat. Commun.* 11:5481.

Li, J., Wang, H., and Li, D. (2020). Self-trapped excitons in two-dimensional perovskites. *Front. Optoelectron.* 13:225–234. doi: 10.1007/s12200-020-1051-x

Li, S., Luo, J., Liu, J., and Tang, J. (2019). Self-trapped excitons in all-inorganic halide perovskites: fundamentals, status, and potential applications. *J. Phys. Chem. Lett.* 10, 1999–2007. doi: 10.1021/acs.jpclett.8b03604

Li, T., Chen, X., Wang, X., Lu, H., Yan, Y., Beard, M. C., et al. (2019). Origin of broad-band emission and impact of structural dimensionality in tin-alloyed Ruddlesden–Popper hybrid lead iodide perovskites. *ACS Energy Lett.* 5, 347–352. doi: 10.1021/acsenergylett.9b02490

Lin, R., Xiao, K., Qin, Z., Han, Q., Zhang, C., Wei, M., et al. (2019). Monolithic all-perovskite tandem solar cells with 24.8% efficiency exploiting comproportionation to suppress Sn (ii) oxidation in precursor ink. *Nat. Energy* 4, 864–873. doi: 10.1038/s41560-019-0466-3

Milot, R. L., Eperon, G. E., Snaith, H. J., Johnston, M. B., and Herz, L. M. (2015). Temperature-dependent charge-carrier dynamics in $CH_3NH_3PbI_3$ perovskite thin films. *Adv. Funct. Mater.* 25, 6218–6227. doi: 10.1002/adfm.201502340

Noh, J. H., Im, S. H., Heo, J. H., Mandal, T. N., and Seok, S. I. (2013). Chemical management for colorful, efficient, and stable inorganic–organic hybrid nanostructured solar cells. *Nano Lett.* 13, 1764–1769. doi: 10.1021/nl400349b

Norris, D. J., Efros, A. L., and Erwin, S. C. (2008). Doped nanocrystals. *Science* 319, 1776–1779.

Parkinson, P., Lloyd-Hughes, J., Gao, Q., Tan, H. H., Jagadish, C., Johnston, M. B., et al. (2007). Transient terahertz conductivity of GaAs nanowires. *Nano Lett.* 7, 2162–2165. doi: 10.1021/nl071162x

Protesescu, L., Yakunin, S., Bodnarchuk, M. I., Krieg, F., Caputo, R., Hendon, C. H., et al. (2015). Nanocrystals of cesium lead halide perovskites (CsPbX3, X= Cl, Br, and I): novel optoelectronic materials showing bright emission with wide color gamut. *Nano Lett.* 15, 3692–3696. doi: 10.1021/nl5048779

Richter, C., and Schmuttenmaer, C. A. (2010). Exciton-like trap states limit electron mobility in TiO_2 nanotubes. *Nat. Nanotechnol.* 5, 769–772. doi: 10.1038/nnano.2010.196

Schubert, E. F. (2015). *Doping in III-V Semiconductors*. Cambridge: Cambridge University Press.

Smith, I. C., Hoke, E. T., Solis-Ibarra, D., Mcgehee, M. D., and Karunadasa, H. I. (2014). A layered hybrid perovskite solar-cell absorber with enhanced moisture stability. *Angew. Chem.* 126, 11414–11417. doi: 10.1002/ange.201406466

Smith, M. D., and Karunadasa, H. I. (2018). White-light emission from layered halide perovskites. *Acc. Chem. Res.* 51, 619–627. doi: 10.1021/acs.accounts.7b00433

Smith, M. D., Jaffe, A., Dohner, E. R., Lindenberg, A. M., and Karunadasa, H. I. (2017). Structural origins of broadband emission from layered Pb–Br hybrid perovskites. *Chem. Sci.* 8, 4497–4504. doi: 10.1039/c7sc01590a

Thouin, F., Neutzner, S., Cortecchia, D., Dragomir, V. A., Soci, C., Salim, T., et al. (2018). Stable biexcitons in two-dimensional metal-halide perovskites with strong dynamic lattice disorder. *Phys. Rev. Mater.* 2:034001.

Ulbricht, R., Hendry, E., Shan, J., Heinz, T. F., and Bonn, M. (2011). Carrier dynamics in semiconductors studied with time-resolved terahertz spectroscopy. *Rev. Modern Phys.* 83:543. doi: 10.1103/revmodphys.83.543

V Laarhoven, H., Flipse, C. F., Koeberg, M., Bonn, M., Hendry, E., Orlandi, G., et al. (2008). On the mechanism of charge transport in pentacene. *J. Chem. Phys.* 129:044704.

Wang, F., Shan, J., Islam, M. A., Herman, I. P., Bonn, M., and Heinz, T. F. (2006). Exciton polarizability in semiconductor nanocrystals. *Nat. Mater.* 5, 861–864. doi: 10.1038/nmat1739

Wang, N., Cheng, L., Ge, R., Zhang, S., Miao, Y., Zou, W., et al. (2016). Perovskite light-emitting diodes based on solution-processed self-organized multiple quantum wells. *Nat. Photonics* 10, 699–704.

Wang, X., Meng, W., Liao, W., Wang, J., Xiong, R.-G., and Yan, Y. (2019). Atomistic mechanism of broadband emission in metal halide perovskites. *J. Phys. Chem. Lett.* 10, 501–506. doi: 10.1021/acs.jpclett.8b03717

Wehrenfennig, C., Eperon, G. E., Johnston, M. B., Snaith, H. J., and Herz, L. M. (2014). High charge carrier mobilities and lifetimes in organolead trihalide perovskites. *Adv. Mater.* 26, 1584–1589. doi: 10.1002/adma.201305172

Yu, J., Kong, J., Hao, W., Guo, X., He, H., Leow, W. R., et al. (2019). Broadband extrinsic self-trapped exciton emission in Sn-doped 2D lead-halide perovskites. *Adv. Mater.* 31:1806385. doi: 10.1002/adma.201806385

Yuan, M., Quan, L. N., Comin, R., Walters, G., Sabatini, R., Voznyy, O., et al. (2016). Perovskite energy funnels for efficient light-emitting diodes. *Nat. Nanotechnol.* 11, 872–877.

Zhang, Q., Ji, Y., Chen, Z., Vella, D., Wang, X., Xu, Q.-H., et al. (2019). Controlled aqueous synthesis of 2D hybrid perovskites with bright room-temperature long-lived luminescence. *J. Phys. Chem. Lett.* 10, 2869–2873. doi: 10.1021/acs.jpclett.9b00934

Conflict of Interest: The authors declare that the research was conducted in the absence of any commercial or financial relationships that could be construed as a potential conflict of interest.